RAPID VARIATIONS OF Si IV LINE PROPERTIES IN AN M-CLASS FLARE OBSERVED BY IRIS AT VERY HIGH CADENCE

Juraj Lorincik[1,2], Vanessa Polito[1,2,3], Bart De Pontieu[2,4,5]
Sijie Yu[6], Nabil Freij[1,2]

1- Bay Area Environmental Research Institute
2- Lockheed Martin Solar & Astrophysics Laboratory
3- Department of Physics, Oregon State University
4- Institute of Theoretical Astrophysics, University of Oslo
5- Rosseland Centre for Solar Physics, University of Oslo
6- Center for Solar-Terrestrial Research, New Jersey Institute of Technology

Hinode-15/IRIS-12 meeting, 2022 September 19 – 23, Prague

Si IV spectra in IRIS flare observations

- Usually redshifts or red-wing enhancements tracing downflows induced by chrom. condensation (e.g. Tian et al. 2015)
- Jeffrey et al. 2018:
  - 2016 Dec 6 B-class flare
  - quasi-periodic broadening in a ribbon (left figure), *P* = 11.5 s
  - oscillations prior to the peak of the intensity, unrelated to the evaporation
  - MHD turbulence developing in the lower atmosphere at flare onset
  - see also Kontar et al. 2017
- Chitta & Lazarian 2020:
  - microflares on 2014 May 25, 2016 July 18
  - quasi-periodicities in excess line width and intensity (right figure)
  - turbulence driving (fast) magnetic reconnection

from Chitta et al. 2020

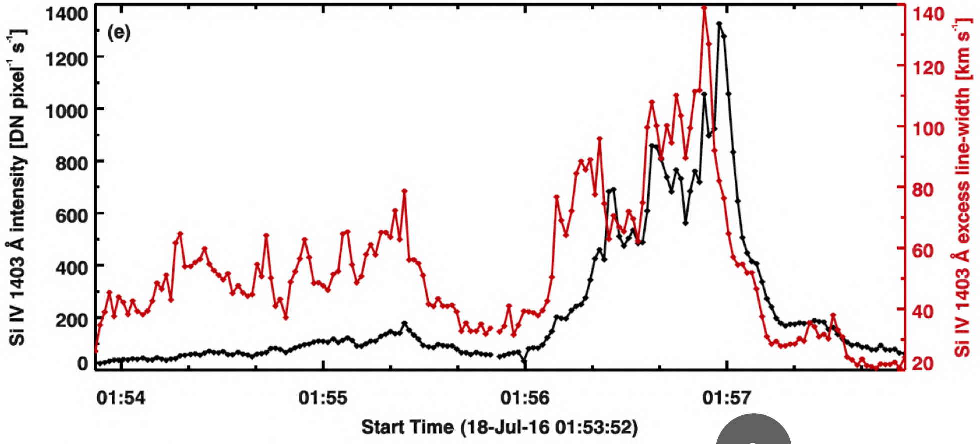

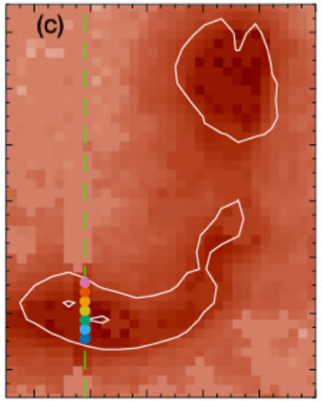

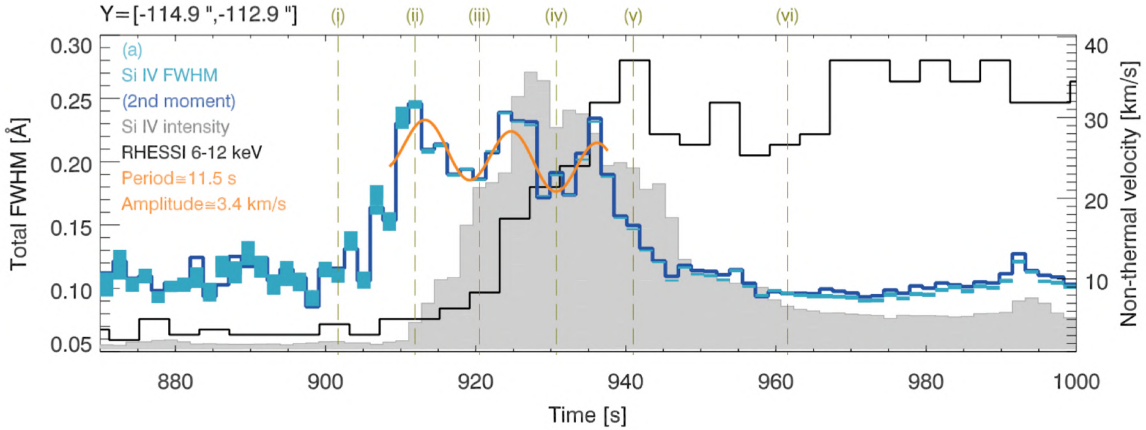

from Jeffrey et al. 2018

2022 January 18 M-class flare

- Interface Region Imaging Spectrograph (De Pontieu et al. 2014, 2021)
- **High priority IRIS science target since Fall 2021: flare observations at sub-second cadence**
- 2022 January 18 M1.5-class flare: the first major flare observed in high-cadence mode
  sit and stare mode, 0.8 s raster & SJI cadence, 0.3 s exposure time
  C II 1336, Si IV 1403, Mg II k 2796, 2814 spectral windows

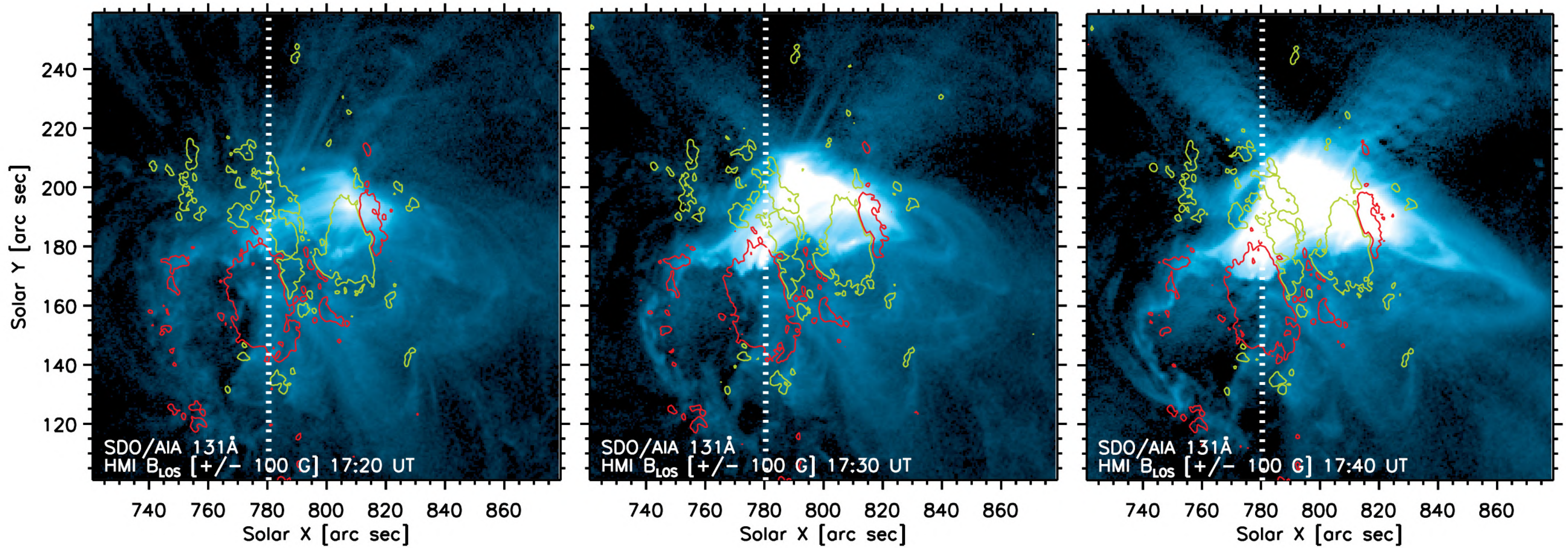

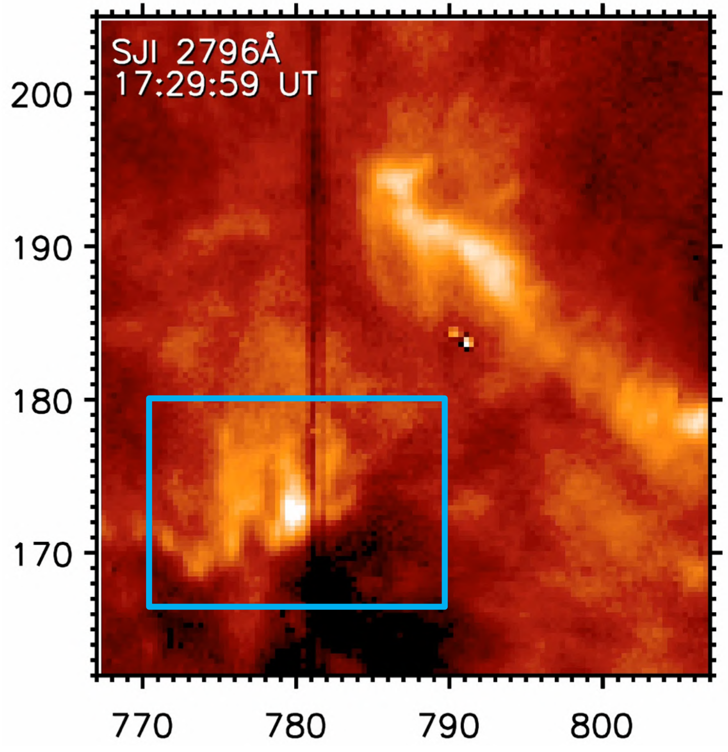

- Two-ribbon flare, southern ribbon under slit, bright kernels from E to W after 17:33 UT

• Maps of Si IV 1402.77Å line moments

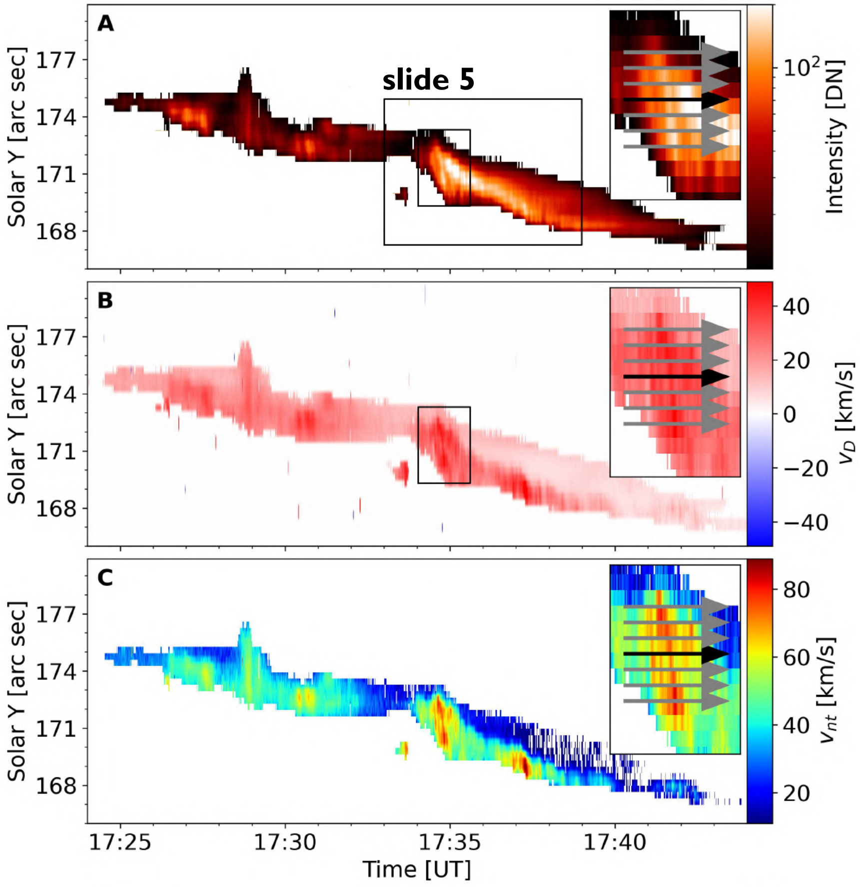

- Maps (Solar Y vs. t) of Si IV properties resulting from moment analysis:
  1) intensity (top)
  2) Doppler velocity v_D (middle)
  3) non-thermal broadening v_{nt} (bottom)
- Arrows: time evolution of the Si IV properties along selected Y-pixels during their initial growth
- High-frequency enhancements ($P < 10$ s) of the 3 properties

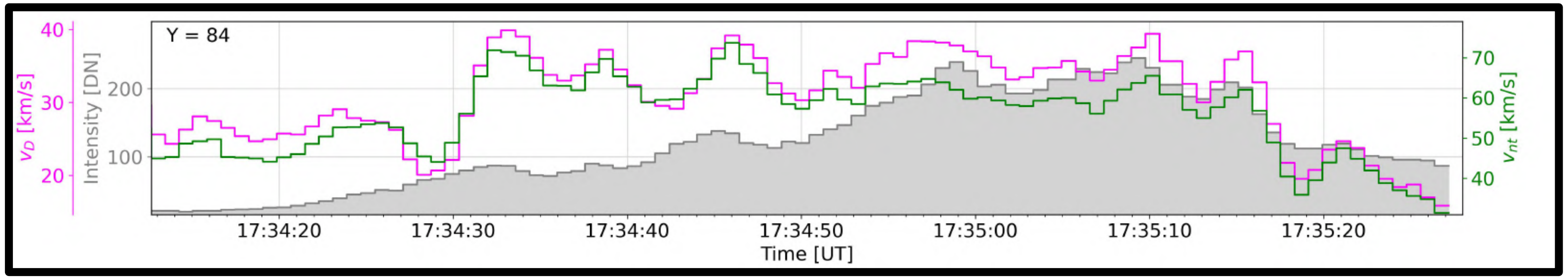

- **The oscillations do not have a counterpart in imaging observations**
- *What is driving them?*

Double-peaked Si IV line profiles

- k-means clustering:
  ca. 35% profiles in the analyzed period exhibited secondary redshifted component
- Strong red wing of the line (RG #9, 12, 29)
- Large separation between the components (RG #18) up to 60 km/s
- Mostly during the period of the initial growth of the 3 parameters of the Si IV line

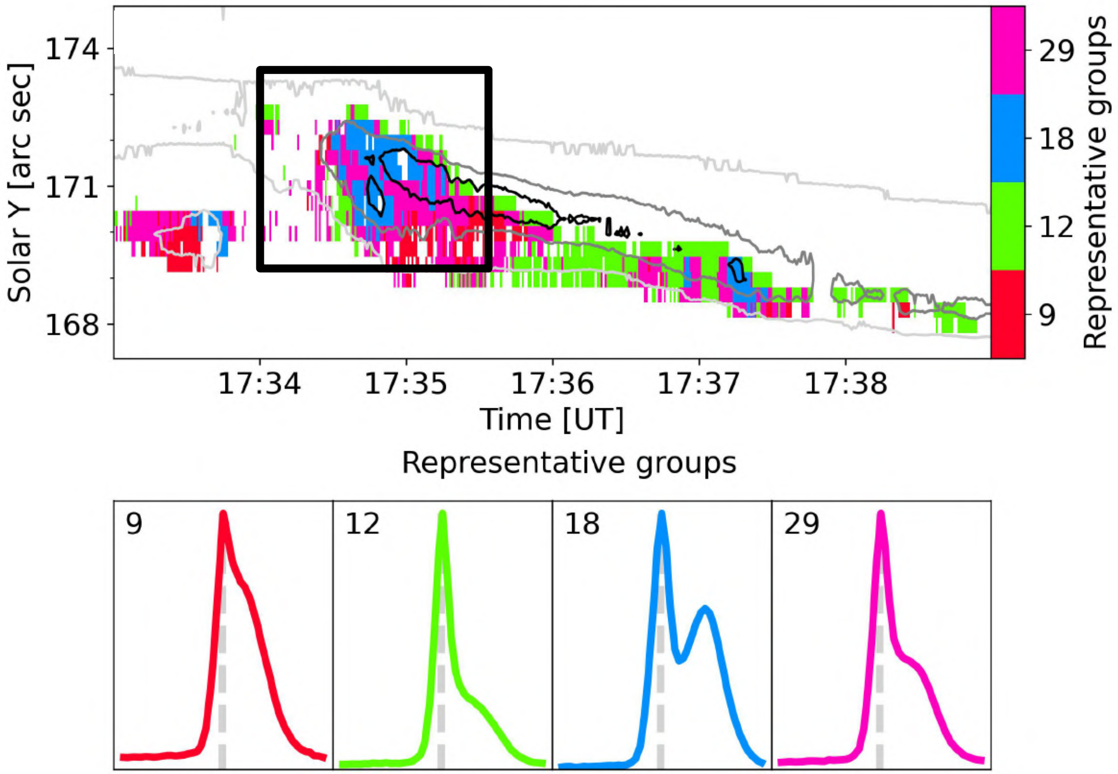

- Note that IRIS flare observations rarely report on:

1. So large separation of Si IV components
2. Secondary component redshifts to more than 50 km/s

- Profiles similar to RG #18 reported e.g. by Brannon et al. 2015

Two-Gaussian fits to Si IV spectra

- G1 fitting the primary component
- G2 fitting the redshifted component

- Figure: time evolution of the Gaussian
  1) intensity
  2) Doppler velocity v_D
  3) non-thermal broadening v_{nt}

- Redshifts of G2 reach up to 70 km/s

2G fits:

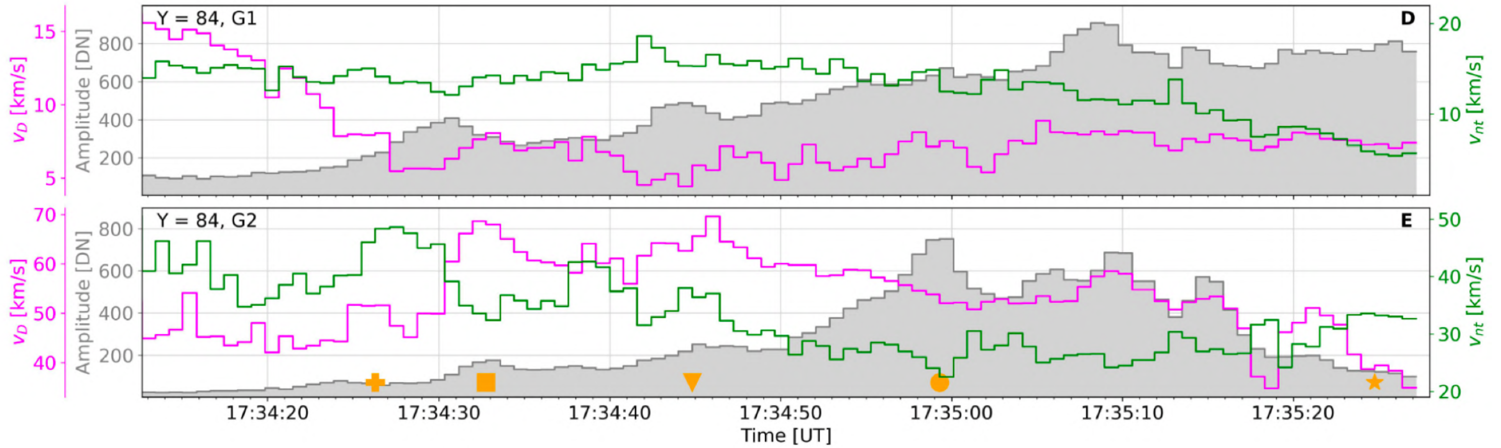

moment analysis (slide 4):

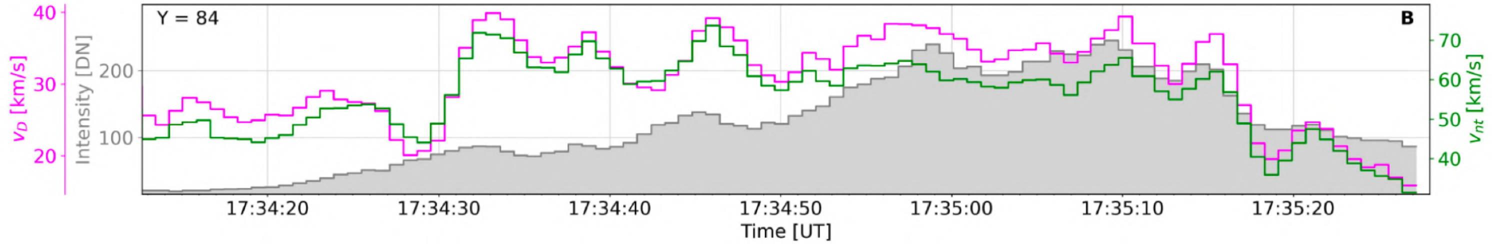

Two-Gaussian fits to Si IV spectra

- G1 fitting the primary component
- G2 fitting the redshifted component
- Figure: time evolution of the Gaussian
  1) intensity
  2) Doppler velocity v_D
  3) non-thermal broadening v_{nt}
- Redshifts of G2 reach up to 70 km/s
- Note the correspondence between the peaks in v_D & amplitude (intensity) of G2 and the entire profile resulting from the moment analysis!

2G fits:

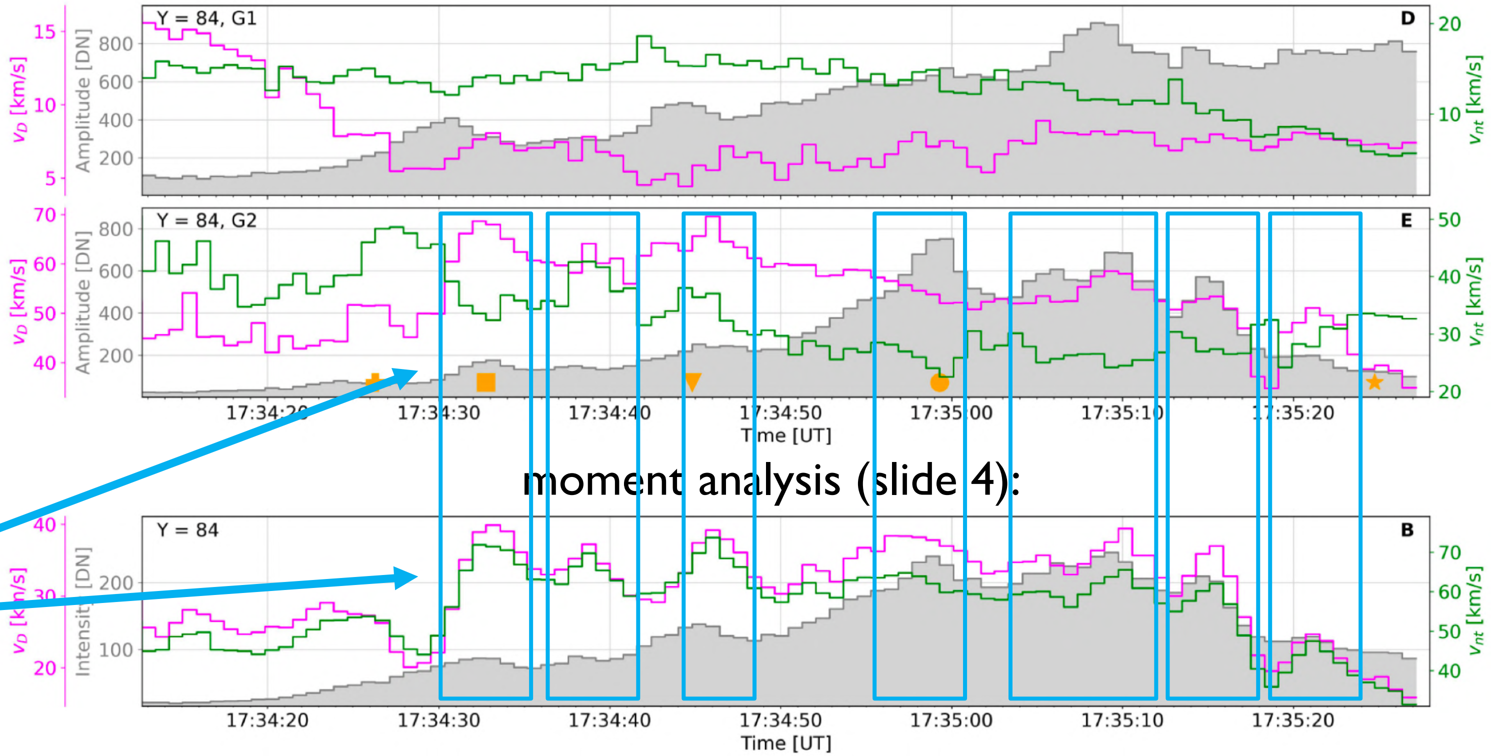

Correlation analysis

- Vertical axis: v_{nt} of the entire profile determined via the moment analysis (MA)
- Horizontal axes: 3 properties of G1 and G2

- v_{nt} (MA) strongly correlated with the Doppler shift of G2
- v_{nt} (MA) only moderately correlated with v_{nt} of G1

- **enhancements of v_{nt} (MA) due to oscillating redshifts of the secondary component of the line and not (only) 'real' broadening of profile**

- Reported at footpoints of coronal loops (De Pontieu & McIntosh 2010)

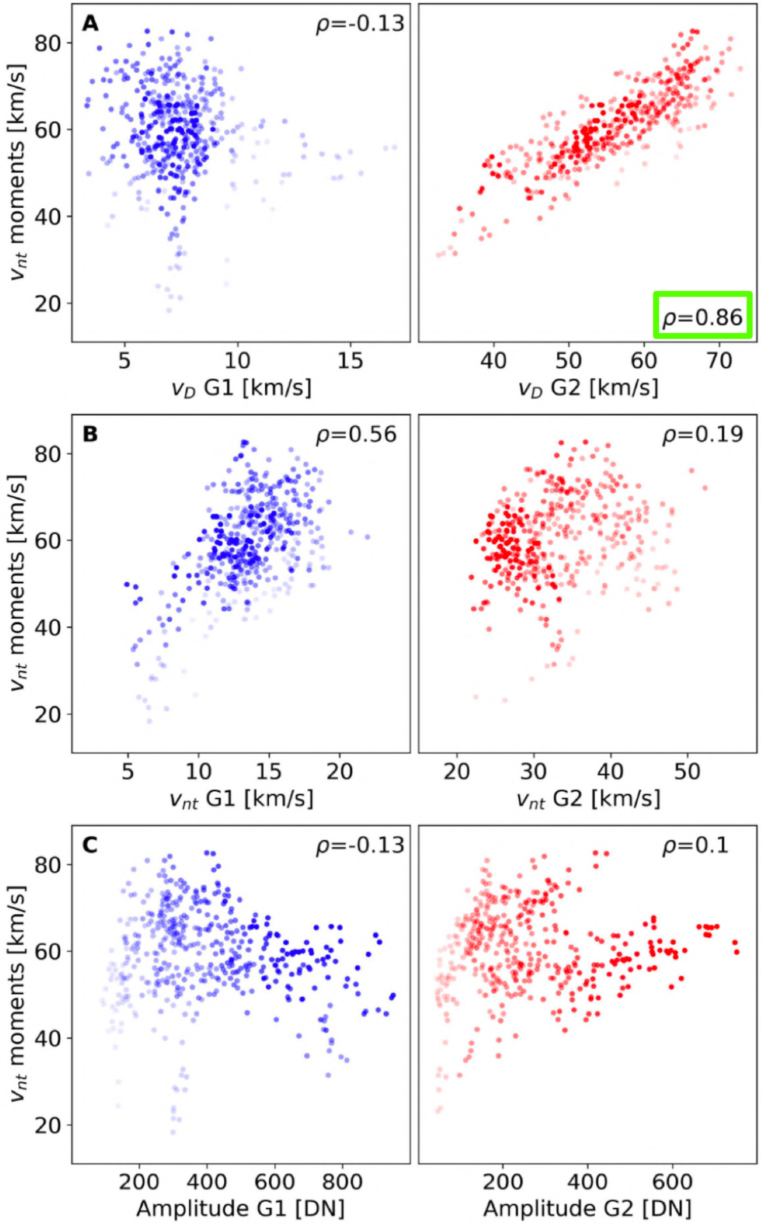

What is the origin of the secondary redshifted component?

- RADYN simulations of Kowalski et al. 2017:
  heating with high non-thermal flux F = 5.10^{11} erg/cm^2/s, δ = 4.2, E_C = 25 keV over 15 s
  2 emitting regions in the chromosphere: condensing layer and stationary layer below it
- Kowalski et al. 2022:
  short-lasting condensation over 100 km/s at maximum gas density
- Our observations: secondary component temporarily redshifted to 70 km/s

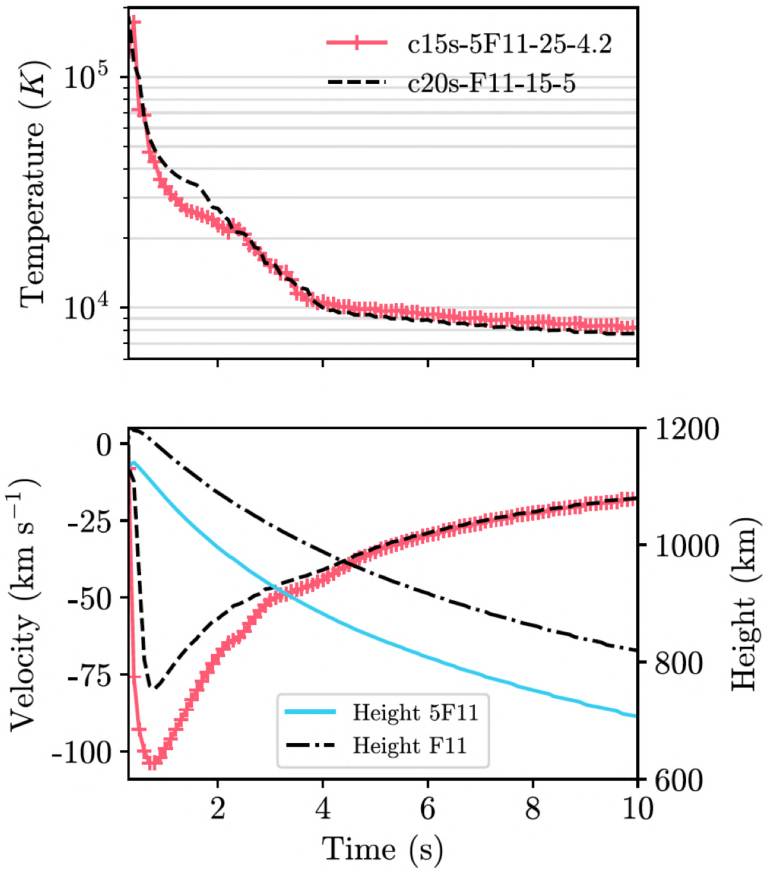

from Kowalski et al. 2022

What is the origin of the secondary redshifted component?

- RADYN simulations of Kowalski et al. 2017:
  - heating with high non-thermal flux $F = 5.10^{11}$ erg/cm^2/s, $\delta = 4.2$, $E_C = 25$ keV over 15 s
  - 2 emitting regions in the chromosphere: condensing layer and stationary layer below it
- Kowalski et al. 2022:
  - short-lasting condensation over 100 km/s at maximum gas density
- Our observations: secondary component temporarily redshifted to 70 km/s

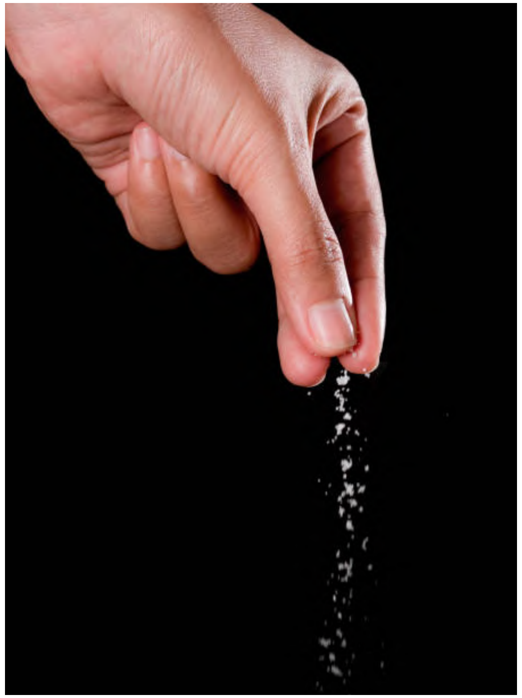

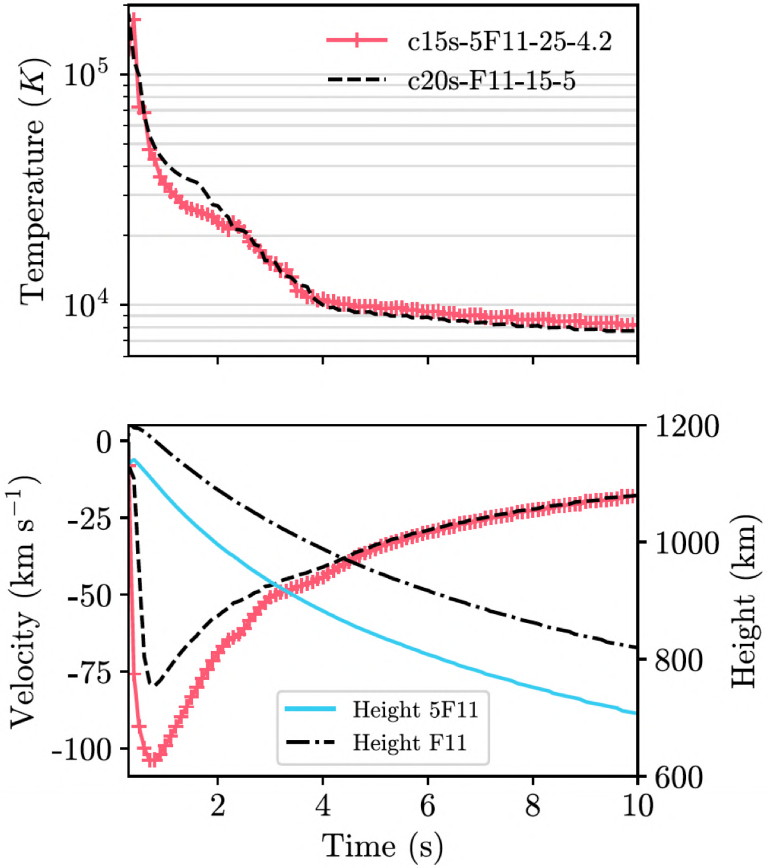

from Kowalski et al. 2022

Estimating field-aligned flow speeds

- *How large would the redshifts be if the flare loops were oriented along the LOS of IRIS?*
- Estimating viewing angle α between the LOS of IRIS and lower segments of flare loops
- 3D flare loop reconstruction using data from AIA and EUVI
- Average loop viewing angle α = 52°

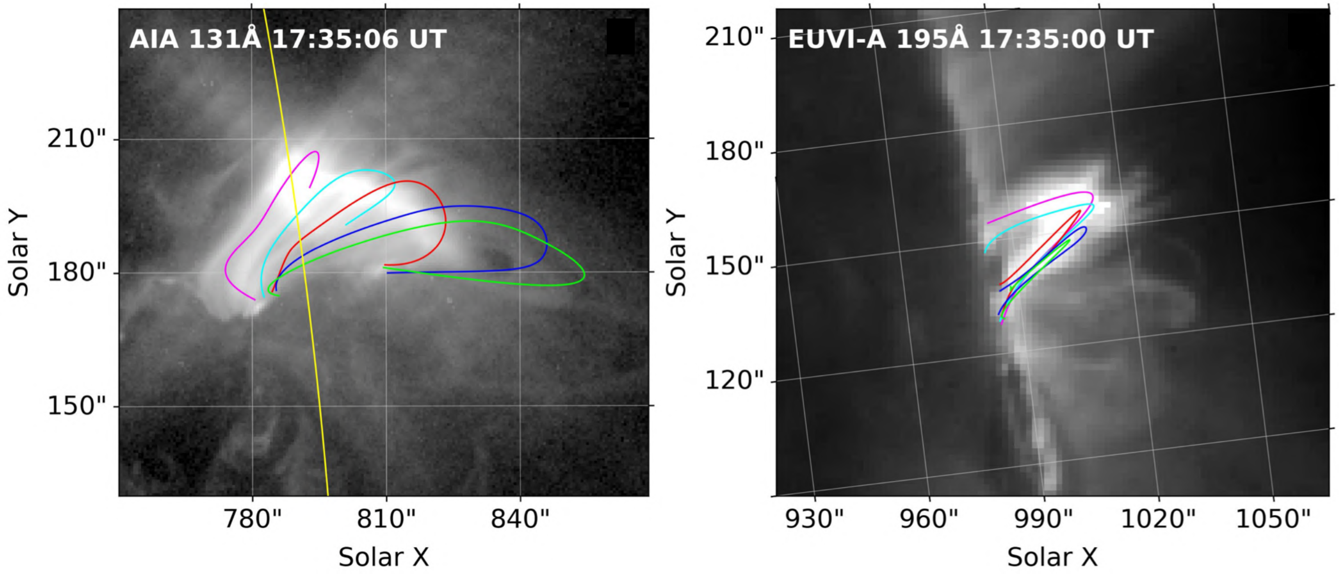

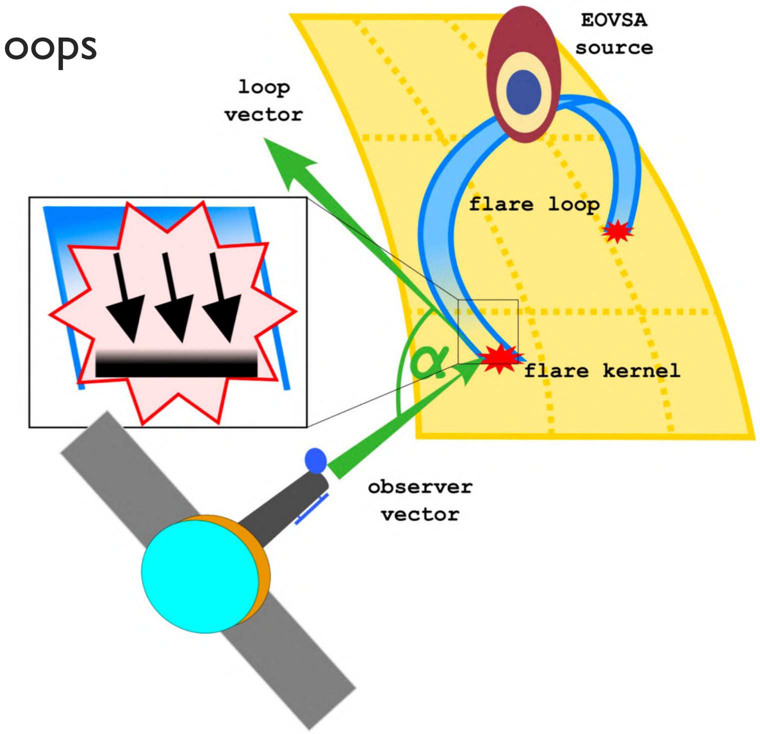

- Field-aligned downflows of 50 – 110 km/s resulting from typical 30 – 70 km/s redshifts of G2
- The secondary component most-likely due to the condensation

sunpy

Microwave & SXR emission during the flare I.

- Microwave emission observed by Expanded Owens Valley Solar Array (EOVSA)
- Sun-as-a-star emission peaked at ~17:37 UT
- Source above the flare loop arcade consistent with CSHKP model
- Brightness temperature spectrum: consistent with non-thermal electron source

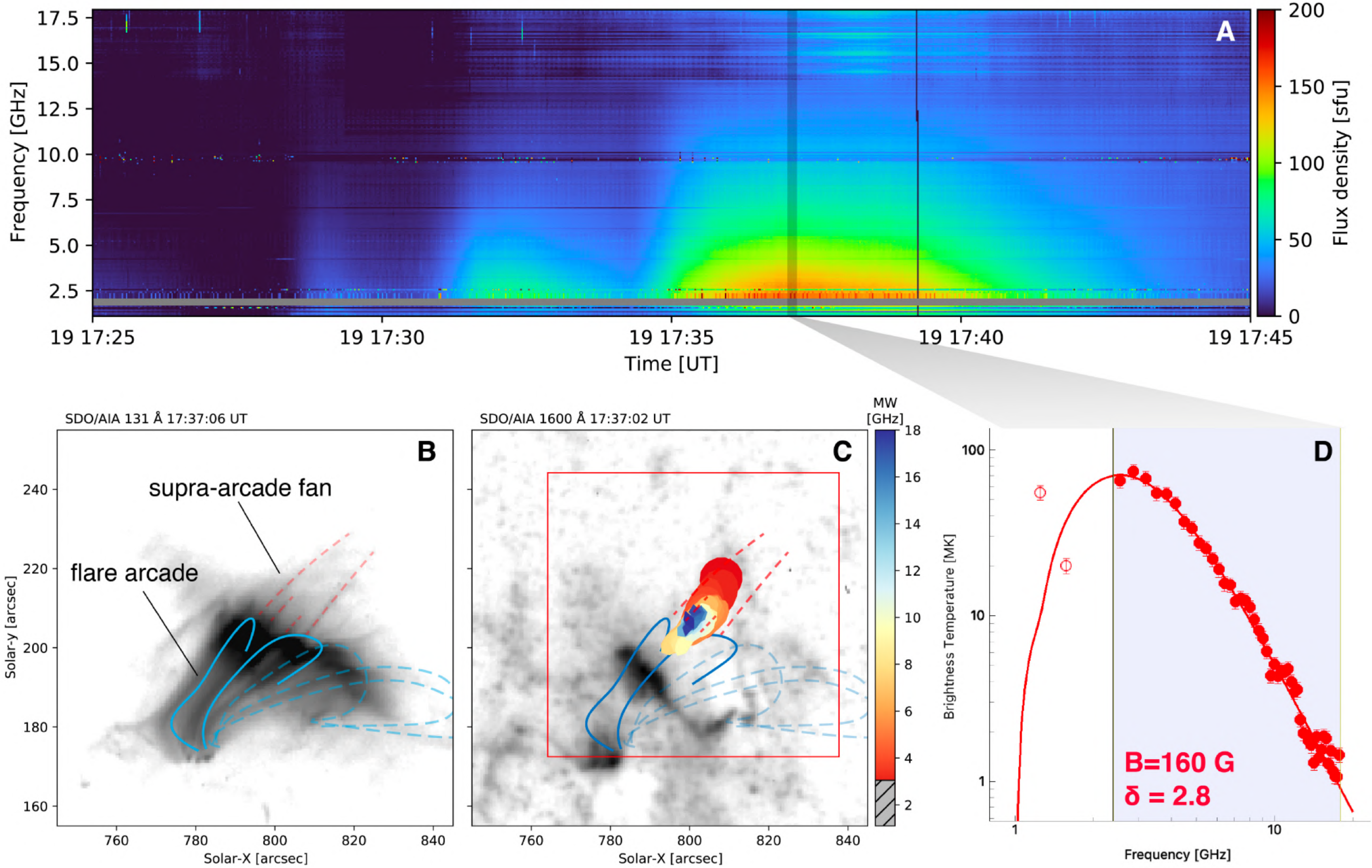

Microwave & SXR emission during the flare II.

- Orange curve: time derivative of microwave flux measured between 2.4 and 5 GHz
- Blue curve: time derivative of SXR flux in 1 – 8 Å channel of GOES
- Quasi-periodic pulsations (QPPs) with period 1 – 3 min
- Si IV fit parameters averaged in the ribbon
- Intensity trend of G2 similar to EOVSA time derivative
- v_D trend of G2 similar to GOES time derivative

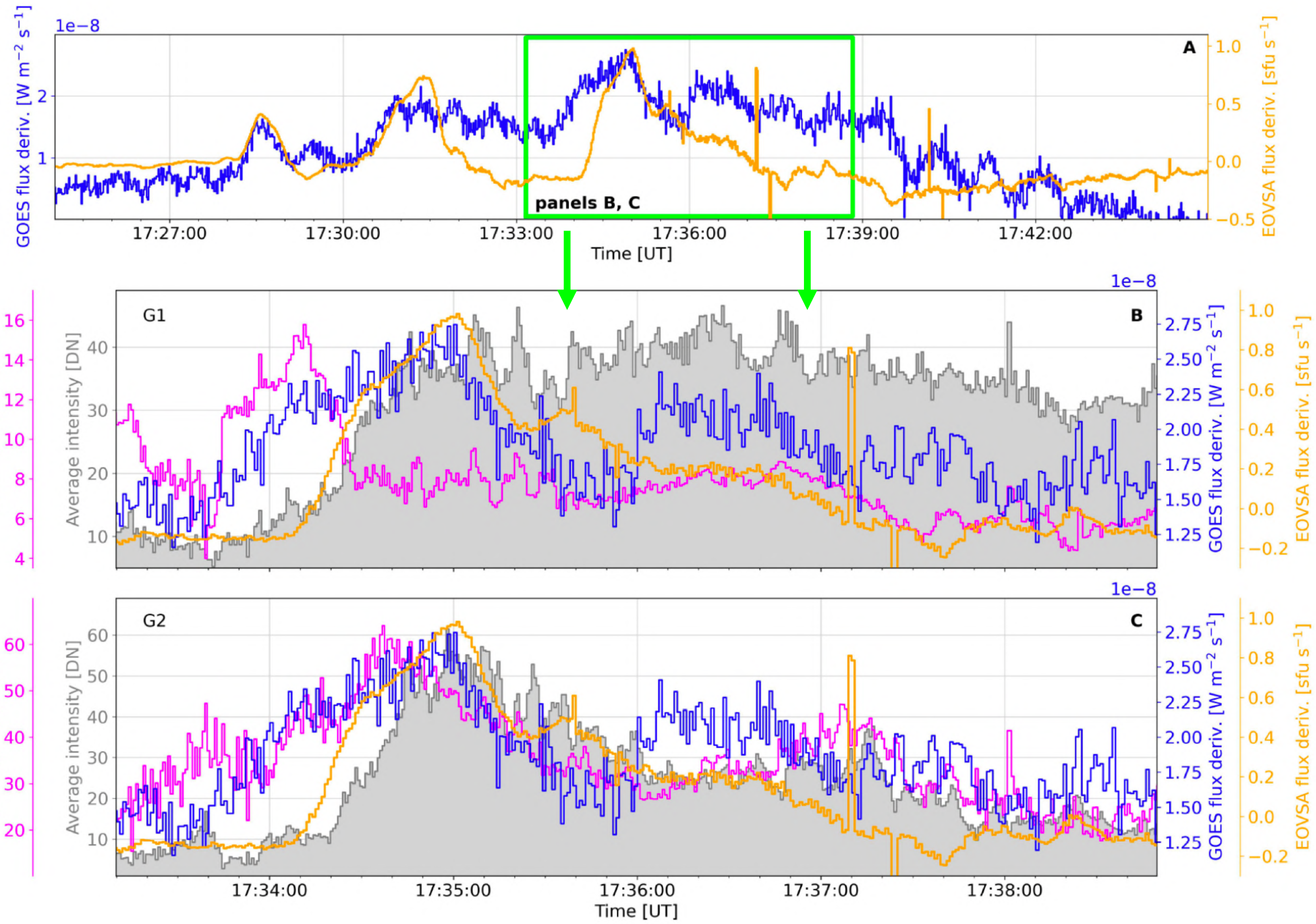

- **Since G2 likely existed due to the chromospheric condensation, QPPs were generated by magnetic reconnection (see also Li, Ning, Zhang 2015)**

Summary

- Si IV 1402.77 Å: quasi-periodic enhancements in moments of the entire profile, no counterpart in imaging data
- Fraction of profiles exhibited two components, primary and secondary one redshifted to ~ 70 km/s
- Very high correlation (ρ = 0.86) between the non-thermal broadening resulting from the moment analysis and the Doppler shift of the Gaussian fitting the secondary component

⇒ **Quasi-periodicities in the broadening of the entire profile due to plasma downflows (manifested in the secondary component) rather than broadening of the profile itself**

- Speeds of the field-aligned downflows obtained by estimating viewing angles of flare loops correspond to high chromospheric condensation speeds recently found in numerical simulations
- Source of EOVSA microwave emission above the flare loop arcade, brightness temperature spectrum consistent with non-thermal electron source
- 1 – 3 minute period QPPs visible in microwave and SXR time derivatives relatable to time evolution of the parameters of the Gaussian fitting the secondary component of the Si IV line

⇒ **QPPs likely induced by magnetic reconnection**

For more details see Lorincik et al. 202X (submitted)
Frontiers research topic: *'Flare Observations in the IRIS Era: What Have We Learned, and What's Next?'*

References

- Brannon, Longcope, Qiu 2015, *ApJ* 810, 4
- Chitta & Lazarian 2020, *ApJL* 890, L2
- De Pontieu & McIntosh 2010, *ApJ* 722, 1033
- De Pontieu et al. 2014, *Sol. Phys*. 290, 2733
- De Pontieu et al. 2021, *Sol. Phys*. 296, 84
- Jeffrey et al. 2018, *Sci. Adv*. 4 2794
- Kontar et al. 2017, *Phys. Rev. Lett.* 118, 155101
- Kowalski et al. 2017, *ApJ* 836, 12
- Kowalski et al. 2022, *ApJ* 928, 190
- Li, Ning, Zhang et al. 2015, *ApJ* 807, 72
- Lorincik et al. 202X, *Frontiers*, submitted
- Tian et al. 2015, ApJ, 811, 139